EXAMENSARBETE I GEOLOGI VID LUNDS UNIVERSITET

Kvartärgeologi

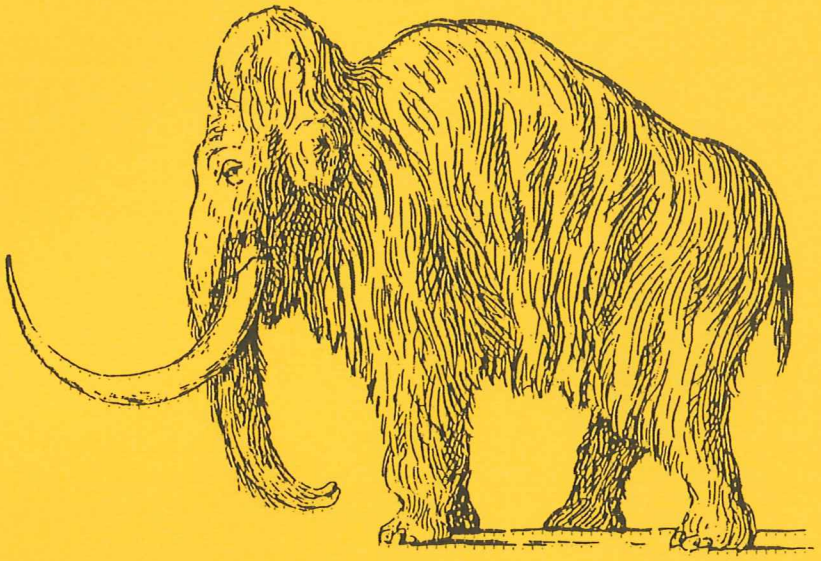

Anti-slope scarp investigation at Handcar Peak, British Columbia, Canada

Magnus Lund

Examensarbete, 20 p
Institutionen, Lunds Universitet

Nr 155

CODEN: SE-LUNBDS/NBGO-02/5155+28S

EXAMENSARBETE I GEOLOGI VID LUNDS UNIVERSITET

Kvartärgeologi

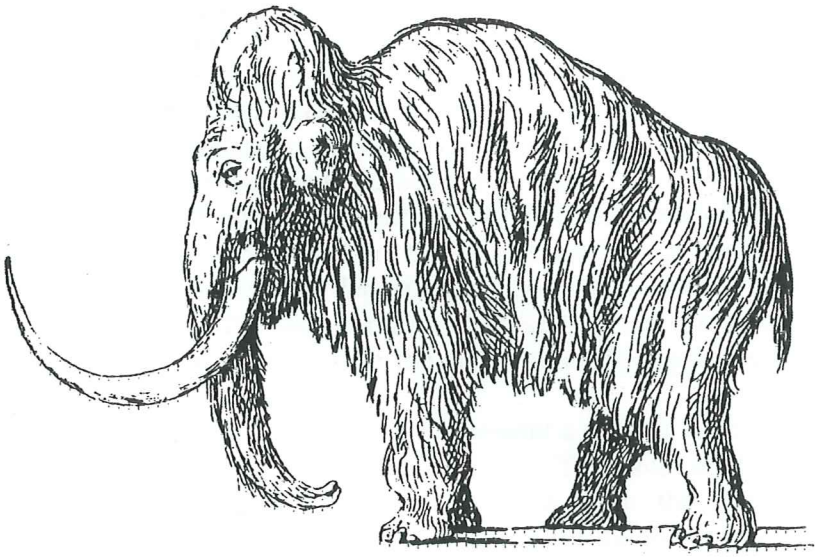

Anti-slopes scarp investigation at Handcar Peak, British Columbia, Canada

Magnus Lund

Lund 2002 **Examensarbete, 20 p** **Nr 155**
Geologiska Institutionen, Lunds Universitet

Anti-slope scarp investigation at Handcar Peak, British Columbia, Canada

MAGNUS LUND

Lund, M., 2002: Anti-slope scarp investigation at Handcar Peak, British Columbia, Canada. Examensarbete i geologi vid Lunds Universitet. 20 poäng. Nr 155, pp. 1 – 28.

Several parallel linear ridges run perpendicular to the slope direction in the high-altitude mountain of Handcar Peak, British Columbia, Canada. The ridges have scarps facing the hillside.

An investigation of one of the anti-slope scarps was made. The main purpose was to investigate the sediments in the depression inside the scarp, and to find a possible cause for these features. Therefore a trench was excavated in the depression towards the scarp. The area was also investigated by aerial photographs and ground penetrating radar. The sediments in the trench were described and interpreted. The floor of the trench consists of weathered bedrock partly altered into clay minerals, which were investigated by x-ray diffraction. A shear zone borders the trench in the southwest. Three sedimentary units were recognised in the trench section; a basal till on top of the saprolite, rock fall and debris flow deposits with a palaeosol, and as the uppermost unit, a fine-grained fluvial sand. The sand contains reworked tephra, which was investigated in a polarizing microscope in order to date the sediments. The tephra belongs to the Bridge River eruption, dated to 2.4 ka BP.

The scarp and the shear zone represent a normal fault. During shearing, the sediments were deformed in a monoclinal bend. The fault is thus very young, and occurred long after the glacial isostatic rebound from the last glaciation, Frasier glaciation. The most possible triggering mechanism for the formation of the scarp was an earthquake related to movement along the edge of the North American Plate.

Keywords: Anti-slope scarp, aerial photographs, ground penetrating radar, tephra, clay mineralogy.

Magnus Lund, Department of Geology – Quaternary Geology, Lund University, Sölvegatan 13, SE-223 62 Lund, Sweden.

Undersökning av ett hak med brant lutning mot sluttningen vid Handcar Peak i British Columbia, Kanada

MAGNUS LUND

Lund, M., 2002: Undersökning av ett hak med brant lutning mot sluttningen vid Handcar Peak i British Columbia, Kanada. Examensarbete i geologi vid Lunds Universitet. 20 poäng. Nr 155, pp 1 – 28.

Flera parallella ryggar korsar sluttningen i de höga bergen vid Handcar Peak i British Columbia, Kanada. Dessa ryggar är hak med brant lutning in mot sluttningen. En undersökning av ett hak genomfördes. Huvudsyftet med undersökningen var att undersöka sedimenten i svackan mellan haket och sluttningen och presentera en möjlig förklaring till dess uppkomst. Därför grävdes en skärning i svackan, upp mot haket. Området undersökes även med hjälp av flygfotografier samt med markpenetrerande radar. Sedimenten beskrevs och tolkades. Botten av skärningen utgörs av berggrund delvis vittrad till lermineral, som analyserades med röntgendiffraktion. Ett skjuvplan utgör skärningens gräns i dess södra del. Tre lager identifierades i skärningen: en bottenmorän på den vittrade berggrunden, rasmaterial och en debris flow-avlagring med paleosol, samt ett lager med fluvialt avlagrad sand. Sanden bestod delvis av omlagrad tefra, vilken undersökes i ett polarisationsmikroskop. Detta gjordes för att datera lagret. Tefran kan knytas till Bridge River-utbrottet som skedde 2.4 ka BP.

Haket och skjuvplanet utgör en normal förkasting. Sedimenten deformerades monoklinalt under skjuvningen. Förkastningen är mycket ung och bildades efter den glacialt isostiska upplyftningen efter den senaste glaciationen (Frasier-glaciationen). Den mest troliga mekanismen för bildandet av haket är en jordbävning relaterad till rörelser utmed kanten av den nordamerikanska litosfärsplattan.

Magnus Lund, Department of Geology – Quaternary Geology, Lund University, Sölvegatan 13, SE-223 62 Lund, Sweden.

Index

1. Introduction

Parallel-running bedrock scarps on steep mountainsides have been described from both North America and Europe. The scarps are generally a few metres in height and vary in length from one hundred metres to several kilometres. They do not always show a clear relation to the overall topography of the landscape but in most cases the linear structures are roughly parallel to the topographic contours. The scarps often face upslope and the features are generally referred to as anti-slope scarps.

The scarps are found in high-altitude mountains, generally above the tree line. They occur in areas that have been exposed to glaciation, where valleys display a u-shape and where mountains have a high relief. In Europe the features are located to the Alps (Zischinsky 1969) and the Carpathian Mountains (Jahn 1964). In North America, the anti-slope scarps are found in both Canada (e.g. Thompson *et al.* 1997) and the USA (e.g. Tabor 1971).

1.1. Objectives

This Master's thesis is the product of collaboration between Lund University, Sweden, and Simon Fraser University, Canada. Dr John Clague, professor in Quaternary geology at Simon Fraser University, Vancouver, initiated the investigation. He has carried out research on bedrock scarps for several years and was starting a new study on the scarps at Handcar Peak Mtn north of Vancouver, Canada. The main purpose of this study was to investigate the risk of future landslides.

My part of the project was to investigate the sediments in a small depression behind one of the scarps. The aim of this Master's thesis was to describe the sediments, to suggest which geological processes that may have formed the scarp and the sediments, and to date the course of events.

1.2. Anti-slope scarp theories

Several theories have evolved over time trying to explain the formation of anti-slope scarps. Theories presented in the literature to explain these phenomena include formation by erosion, large-scale gravitational slope processes and neo-tectonics, or a combination of these processes.

After an investigation at Affliction Creek (British Columbia, Canada), Bovis (1982) proposed that anti-slope scarps are formed due to a combination of two processes. The first process is displacements along planes of weakness within the bedrock, which forms a slight notch in the hillside profile. This notch is enlarged by erosion of the uphill faces.

Anti-slope scarps formed in glaciated areas could also be caused by rapid change in the slope stress (Tabor 1971). When the glacier retreated, the steep valley sides were not stable enough and creep was induced, followed by landslides forming the scarps. These large-scale creeps appear to bend steeply dipping stratified or foliated rocks down slope. The scarps occur in areas of high altitude, often above the tree line. When scarps occur below the tree line, Tabor (1971) concluded that these scarps date back to a time when the tree line was lower. The altitude and thereby the severe climate conditions influence the formation of scarps (Tabor 1971). Evans (1987) suggested that tension cracks in the bedrock surface are caused by gravitation. Measurements across these cracks showed a slow and uneven rate of extension, with a constantly increasing width of the cracks (Bovis 1990).

A strictly neo-tectonic origin for anti-slope scarps was suggested by Bell and Eisbacher (1996). The linearity of the scarps and their relation to pre-existing tectonic zones were used as arguments for displacements along deep-seated crustal fractures.

When Thompson *et al.* (1997) excavated a trench across a scarp in the southern parts of Coast Mountain, they identified at least three periods of bedrock activity, dating from late Pleistocene to late Holocene time. At the same location, they observed that movement had occurred along near-vertical shear zones being pre-existing planes of weakness in the bedrock. The tilted and warped sediments at the site provided evidence both for gravitational deformation and tectonic movement. This explains the linearity and geographic distribution of the scarps.

2. Setting

2.1. Geology in the investigated area

The study area is located in the Canadian Cordilleran (Fig. 1). The nearest town is Pemberton, which is situated five kilometres east of the site along the Lillooet River valley and one hundred kilometres north of Vancouver. The Cordilleran Mountain Range is located at the western edge of the North American lithospheric plate along a northward strike-slip fault. The processes along the fault have given the Cordilleran a strong northwest – southeast structure. Due to the fault, there is also a complex distribution of rocktypes within the region (Clague 1989). The Coast Belt is situated in the western part of the Cordilleran Mountains. The Coast Belt is divided into three parts: the Western, the Central and the Eastern Coast Belt. The southern part of the Coast Belt is underlain by a granitic rock complex, called the Coast Plutonic complex (Friedman *et al.* 1995).

The Western Coast Belt extends from the coast and continues 150 km eastward into the mountains, where it meets the Central Coast Belt. The investigated site is located in the Western Coast Belt, close to the border to the Central Coast Belt. The intrusion that forms the bedrock at the site is a lecocratic biotite tonalite/granodioritic body called the Lillooet River tonalite/granodiorite intrusion (Friedman *et al.* 1995). The Lillooet River tonalite/granodiorite intrusion has a triangular shape. The late Triassic Cadwallader Group is situated towards the northeast and Cenozoic sediments are formed to the south. To the west lies a pluton of unknown age. The border to the late Triassic Cadwallader Group is formed by a thrust-reverse fault. This fault is part of the Coast Belt thrust system and runs in a northwest – southeast direction. U-Pb analyses show that the Lillooet River tonalite/granodiorite have an age of 110.45±2.65 Ma and $^{207}Pb/^{206}Pb$ analyses indicate an age of 111±14 Ma (Friedman *et al.* 1995). The bedrock in the investigated area is generally granodiorite, which is very common in the Coast Mountains as a whole.

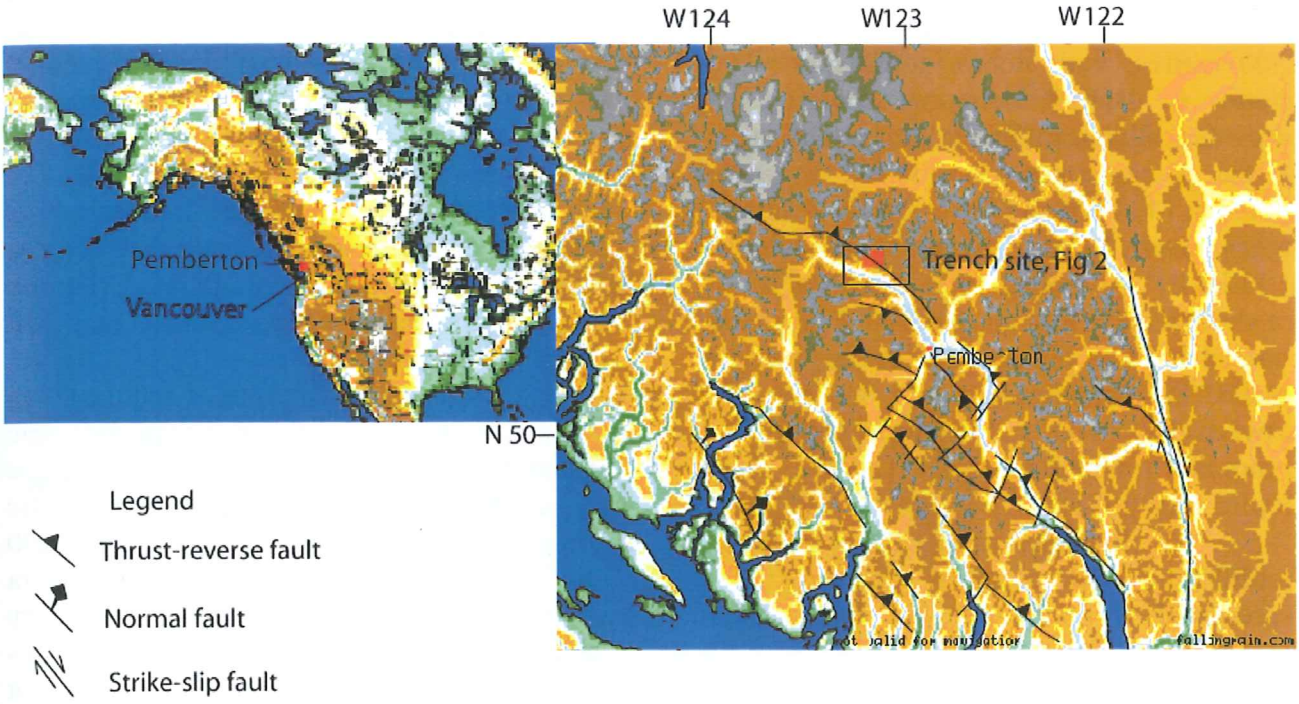

Figure 1. The location of the investigated area.

2.2. Neo-tectonic activity in the Canadian Cordilleran

The present tectonic regime of western North America is controlled mainly by the motions of the Pacific, the North American and Juan de Fuca plates. Many faults in the Canadian Cordilleran are presently active or have been active at some time during the Holocene (Clague 1989).

Magnitude 5,0-5,5 earthquakes have been recorded in the southern Coast Mountains on at least four occasions in the beginning of the twentieth century. The latest earthquake in the area was in 1968, when a magnitude 4,5 earthquake struck the region with a centre just 100 km northwest of the town Pemberton in the southern Coast Mountains. None of the faults in the region are known to be active today, but faults in the northern Cascade Range of Washington, as well as in the southern parts of Coast Mountains, have been closely investigated for their seismic potential. Holocene earthquakes as large as magnitude 8+ have been shown to occurred in southern British Columbia (Clague *et al.* 1998).

2.3. Quaternary geology of the Canadian Cordilleran

The last major glaciation in the area was the Frasier glaciation. The Frasier glaciation occurred during the Late Wisconsinan substage (Ryder *et al.* 1991) and started at 28 ka BP. During the first 10 ka of the Frasier glaciation the ice sheet remained within the mountains, but during the following 8 ka the ice expanded into the lowlands. The Cordilleran Ice Sheet reached its maximum in the south during the peak of the Frasier

glaciation at 14 – 14,5 ka BP (Ryder *et al.* 1991). The ice thickness was approximately 2500 metres, with domes formed over the interior of British Columbia covering the entire Cordilleran Mountain range. The decay of the southwestern Cordilleran Ice Sheet started at 14 ka BP and the coastal lowlands of south-western British Columbia were ice free at 13 ka BP. At around 10 ka BP, most of the ice sheet and satellite glaciers had disappeared completely. The present glaciers in the area reached their maximum during the Holocene between 1500 AD and 1850 AD, a period commonly referred to as the Little Ice Age (Ryder *et al.* 1991).

In many parts of the Canadian Cordilleran, the Frasier glaciation is represented by only one till unit, which sometimes is bounded by stratified units. In some areas the Frasier glacial drifts are more complex and include two or more units of till.

In the southwestern mountain areas of British Columbia, in fjords and valleys parallel to the ice movement all sediments from earlier glaciations were eroded during Frasier glaciation. Older sediments, underlying the Late Wisconsinan glacial deposits, are only found in some parts of British Columbia. Older Pleistocene glacial and non-glacial deposits protected from glacial erosion are found locally beneath the Frasier drift, as well as in lowlands at the periphery of the former ice sheet. This is often the case in places where the ice flow direction was transverse to the valleys. Extensive older deposits have been found on eastern Vancouver Island (N 54° lat., W 126° long.), eastern Graham Island (N 54° lat., W 132.5° long.) and in the Frasier lowlands (Ryder *et al.* 1991). Older sediments can also be found at the surface in the Yukon Territory a thousand kilometres further north, and along the eastern margin of the Cordilleran Mountains and in parts of the continental shelf.

During de-glaciation, sedimentation was located to valleys, lakes and the sea. Many valleys were filled by enormous amount of sediments. The period of rapid aggradation in the valleys was followed by a period of erosion due to the decrease in sediment load of the streams. During middle and late Holocene, the streams had nearly the same discharge as today. Holocene sedimentation has primarily occurred in lakes, seafloor basins, fans and deltas (Clague 1989).

Also other types of sediment can be found in the Canadian Cordillera. Volcanic material such as lava, tephra and coarse pyroclastics of basaltic, andesitic and dacitic composition are found at more than 100 Quaternary eruptive centres. Layers of tephra occur within non-volcanic sedimentary deposits. The tephra particles are of sand-, silt- and clay size. Tephra layers are important even if they generally are very thin. Because the tephras are widespread, and have known ages, they can be used as marker horizons for correlation (Clague 1989).

2.4. Description of the study area

The investigated area is located in the Coast Mountains Pacific Range, in the south-eastern part of British Columbia. The area is approximate 8 x 5,5 kilometres in size and includes the hillside north of Lillooet River valley. Several high mountains are found within the area. The highest nearby mountain peak is Mount Samson located 3500 meters above sea level northeast of the investigated area (Fig. 2). The difference in altitude between the valley and Mount Samson is 2700 meters over a distance of 7 kilometres.

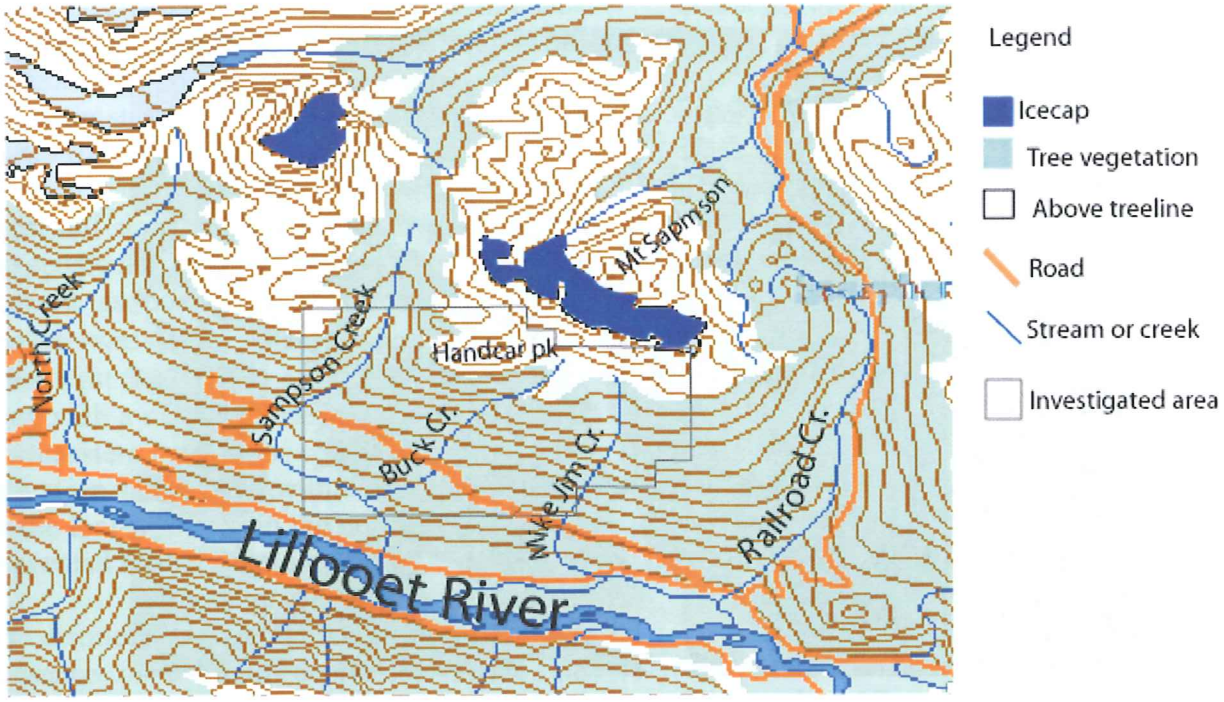

Figure 2. The investigated area.

Other peaks lying more or less in a row north of Lillooet River are Mt Pauline, Locomotive Mtn, Tender Mtn, Caboose Mtn and Handcar Peak Mtn. The bedrock in the area generally consists of a fine grained felsic granite, slightly foliated and light-grey in colour. Locally a greenish rock can be found as bedrock. This is a sedimentary rock with rounded grains of quartz that displays a low grade of metamorphism. The bedrock is dominated by a northwest – southeast trending structure.

At North Creek, just 400 meters from the trench site, several joint-sets have been recorded (M. Bovis pers. com.). The number of sample points was 165 (Fig. 3). The hillside slopes towards south-southwest. The steepest part of this hillside is between 1300 – 2300 meters. A large number of anti-slope scarps are formed in the steep mountain slope.

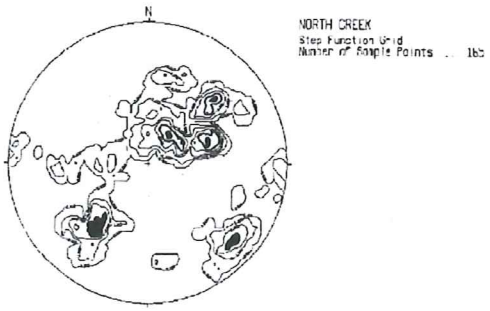

Figure 3. Polepoints of jointsets. Data provided by M. Bovis.

The area is drained by Lillooet River. The trunk valley has an u-shape profile typical for glaciated high-relief mountain environments (Benn and Evans 1998). A number of small canyons have been eroded by streams and creeks on the hillsides.

Figure 4. Scarp with snow in the depression during late July. (Photo Magnus Lund.)

On the map the canyons can be seen along the southern hillside of Handcar Peak Mtn, northwest of where Railroad Creek meets Lillooet River. Several of the creeks come from ice fields lying close to the mountain tops. Other creeks drain small lakes or ponds that have been dammed by anti-slope scarps. Snow tends to lie longer in depressions behind anti-slope scarps (Fig. 4). Many of the ice fields are situated on the northern or north-northeastern side of mountaintops, restricting the number of streams on southern hillsides.

3. Methods

3.1 Aerial photographs

Aerial photographs were used in order to identify anti-slope scarps. The aerial photographs where black and white and covered a 44 km^2 large area along the northern hillside between Railroad Creek and North Creek. The position of the anti-slope scarps were drawn on a map over the area (map no 92J.055 scale 1:20000). Inspection of aerial photographs and maps also gave an overview of the landscape within the study area.

3.2 Field work

3.2.1 Trench excavation

Trench site

A trench was excavated in the uphill face of an anti-slope scarp and into the depression inside the scarp. The trench site is located 1,5 km southeast of Handcar Peak (Fig. 2), one hundred meters above the treeline.

The morphology of the investigated scarp is distinct. The crest of the

low, linear ridge is flat, with angular and sub-angular boulders sparsely scattered on the surface. The depression inside the scarp is approximately 1 m deep and 8 m wide, and partly filled with numerous large boulders.

The scarp runs obliquely to the local hill-slope and the trench was excavated perpendicular to the low ridge and made as straight as possible. The orientation of the trench was from the northeast (32°) to southwest (212°). The excavation was 360 cm long with a maximum depth of 180 cm in the northeastern part. In the south digging stopped at a steep shear-plane with weathered bedrock in the foot-wall, and in the north a big boulder prevented further digging.

The site was chosen because of its distinct upslope facing scarp and the presence of a small depression inside the scarp, which may contain sediments related to the formation of the scarp. Ideally, a trench should be located within an evenly sloping anti-slope scarp showing a visible boundary to the ground at the foot of the scarp. Because the slope and the depression inside the scarp were partly covered with big boulders below the surface, a location with few boulders had to be chosen for the excavation.

Trench excavation and documentation

The trench was oriented in a northeast (032°N) to southwest (212°S) direction perpendicular to the scarp. The trench was 3.6 m long with a maximum depth of 1.8 m in the northern part. Documentation was made for the northern wall. The wall was divided into squares by horizontally and vertically placed cords. The space between cords was 20 cm. Nails with coloured heads were used to mark boundaries between layers. Layers were described on the basis of their texture, colour, sedimentary structures, consistency, boundaries to neighbouring layers, clasts characteristics and other special characteristics within layers. Clast roundness classification was made according to Pettijohn (1975), and clasts were categorised in six classes from very angular to well-rounded. A detailed drawing of the wall was made at a scale of 1:5. Clasts bigger than 5 cm were indicated. The coding of lithofacies was made according to Eyles *et al.* (1983). Photographs were also taken for documentation.

Fabric analysis

Clast orientation data, measured in the field, were statistically evaluated by using the eigenvalue method according to Mark (1973). Fabric analyses were made in a till, 165 cm to the left of 0. The fabric analyses were measured on 17 particles. Measurements were made along the a-axes of the particles, and both the direction and the dip was included. The clasts were collected for shape analysis (Tucker 1981) and origin analysis.

Sampling

A sample was taken for tephra analysis, in the lower parts of unit 3 on the border to unit 2, at 165 cm (Fig. 9). Three clay samples were taken for x-ray diffraction analysis. Two samples were taken in the bottom of the trench and one sample was taken in the shear zone.

Profile of the slope

A 48 metres long profile was made by S. Evans parallel to the trench using a hand clinometre. Another profile, scale 1:5000, was produced based on data from map no 92J.055. The profile was 1850 metres long with an altitude difference of 940 metres.

3.2.2. Ground penetrating radar

Ground penetrating radar (GPR) was use at the trench site. Two radargrams were produced by J. Chow. The radargram record were taken along a section from south towards north, perpendicular to the anti-slope scarp and passing four metres southeast of the trench.

The antenna had a frequency of 200 MHz and the travel time of the signal was 100 nanoseconds. This results in low image resolution but deep penetration of the ground. The reading is longer and penetrates deeper than the excavated trench. One radargram (no. 1538) was 30 metres long and another (no. 1541) was 50 metres long. Both penetrated ten metres into the ground.

3.3 Laboratory methods

3.3.1. Tephra analysis

The sand sample containing tephra was analysed in a polarizing microscope after grinding and addition of an oil with a refractive index of 1.500, which is close to that of glass.

3.3.2. Clay mineral analysis

Samples collected for clay mineral analysis were analysed by x-ray diffraction (XRD) according to the method described by Hardy and Tucker (1988). Four different analyses were preformed on each sample. The first analysis was made on an untreated sub-sample as a reference. The remaining three analyses were made after treatment with heat (550° over night), ethylene glycol (EG) and hydrochloric acid (HCl), respectively. This procedure produced a complete list of the different clay minerals present in the sample. The rationale behind this procedure is that each treatment induces certain clay minerals to change, thereby facilitating interpretation of clay minerals.

Heating to 550° makes the lattice of kaolinite to collapse, resulting in destruction of this clay-mineral. During the EG treatment the sample gets exposed to ethylene glycol vapour for at least four hours, which leads to an expansion of smectite lattices. This can be seen as a peak change compared with the untreated analysis. Chlorite and some smectites are susceptible to acids. Therefore, the HCl-method is used to get rid of some of the clay minerals to facilitate identification.

4. Results

4.1 Distribution and morphology of anti-slope scarps in the area

A series of linear bedrock scarps occur on the mountain slope in the investigated area. The scarps are easily identified on aerial photographs, and they are all roughly parallel, showing the same general northwest – southeast direction (Fig. 5). The scarps on the slope southwest of Handcar Peak follow approximately the topographic contours. However, in the area southeast of the peak the orientation is more oblique to the slope, but the northwest – southeast trend remains the same. About 60 scarps of different size and length were recognised in the area. Most of the scarps are up-slope facing or anti-slope scarps.

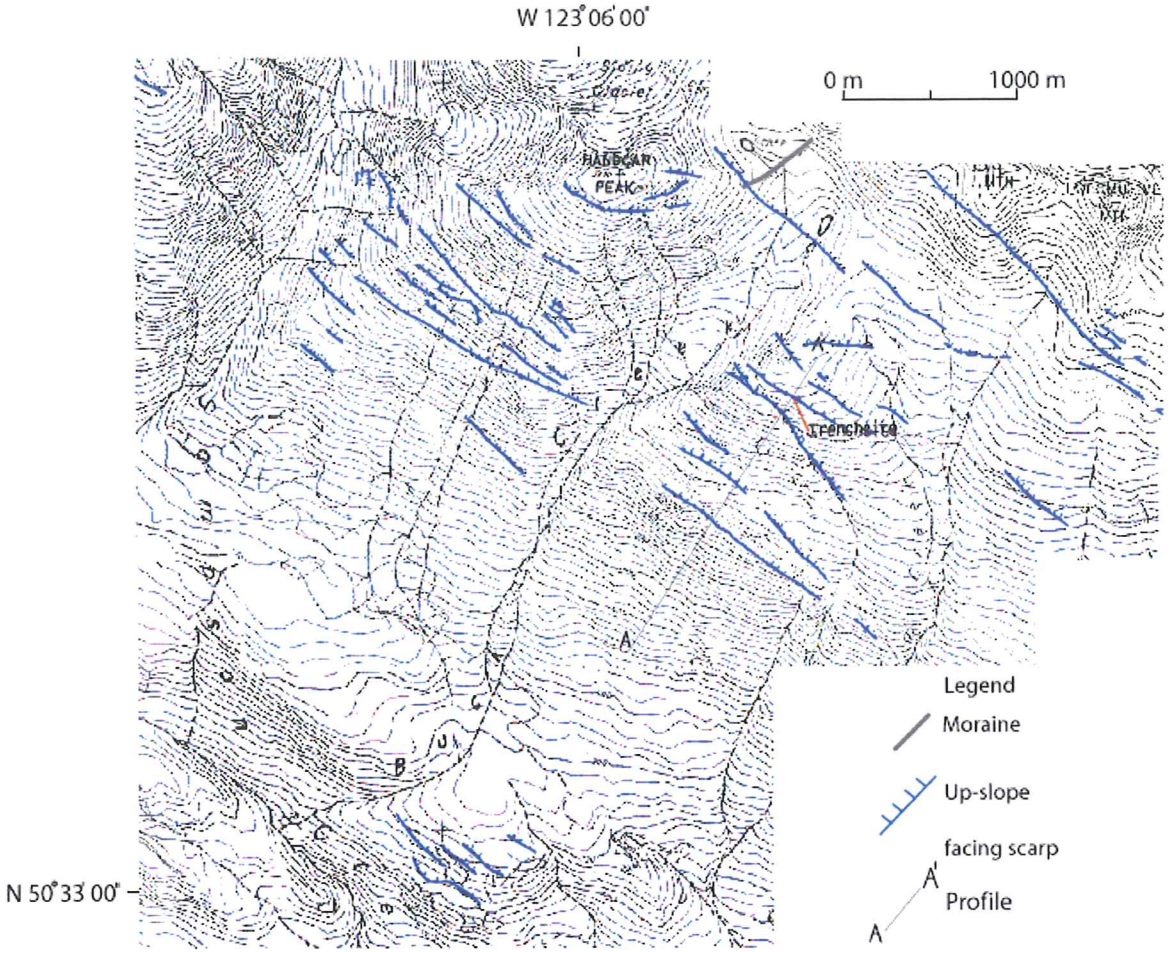

Figure 5. Detailed map over the investigated area. (Map no 92J.055)

The scarps occur along the hillside in the more steep parts. The u-shaped valleys show a relief increase from the bottom of the valley upwards the mountain. This relief increase ceases at high altitude, and the slope decreases out before the mountain top is reached. The most common location for the scarps is just below the less steeper part of the slope (Fig. 5). The scarps occur both beneath and above the tree limit, even if they appear to be less common below.

The anti-slope scarps vary in length from a couple of hundred meters up to 2,1 km within the investigated area. Several anti-slope scarps disappear for a couple of hundred meters and then seem to reappear and continue. There are examples of one anti-slope scarp crossing another. This occurs west of the trench site and at the peak west of Sampson Creek. At the crossing point, both are only seen as slight unconformities on the ground. However, only a few meters from the crossing point, both have grown to their ordinary size as before.

A 600 metres long scarp southwest of Handcar Peak Mtn is, together with the peak, forming a ridge-top depression, or a doppelgrat. A doppelgrat is a scarp running right through a peak, giving the impression of splitting the peak into two (Jahn 1964). The scarp initially trends west-northwest towards east-southeast, making a bend towards the east halfway through its stretch.

An anti-slope scarp crossing a moraine is seen on the aerial photographs 500 metres east of the peak of Handcar Peak. A clear hump has been formed where the scarp crosses the moraine.

At several places the anti-slope scarps are oriented perpendicular to the direction of water transport, resulting in formation of ponds and small lakes. At high altitude the scarps tend to promote accumulation of thick snow in the depressions behind the scarps. These banks of snow presist far into summer (due to their thickness).

Scarps are usually found to be a couple of meters or more as measured from the scarp crest to the bottom of the depression between the anti-slope scarp and the hillside. The larger ones are several tenths of meters wide (Fig. 6 and 7). The crest is rounded on the smaller ones, and on some of the broader anti-slope scarps this is formed as a flat plateau. The ground in the depression behind the anti-slope scarp is generally covered with scattered angular clasts in the size of cobbles or boulders. As indicated by their colour they appear to originate in the higher ground, and they are likely to have been transported by gravitational processes. Moreover, the depressions between the scarps and the slope are filled with various types of sediments. The particles found on the surface are usually made up of fine-grained felsic granite with a slightly foliated texture. The depressions vary in size between a few decimetres to a couple of meters.

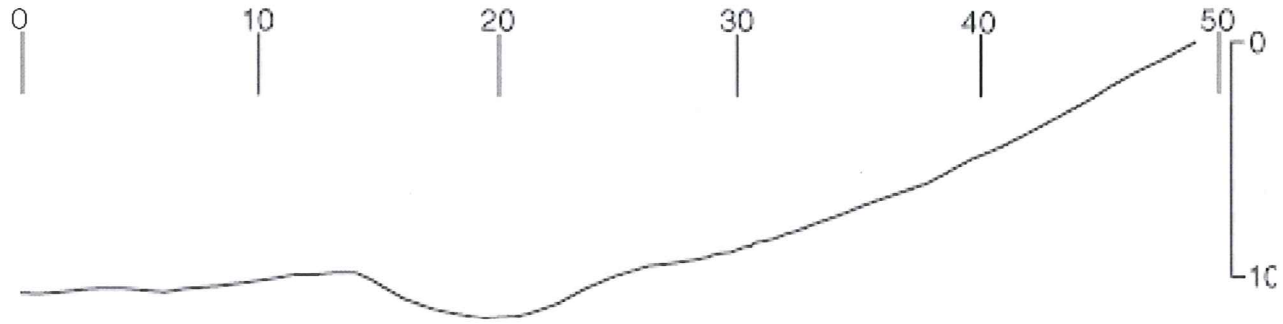

Figure 6. Slope profile across the scarp. All numbers in meters. (by S. Evans.)

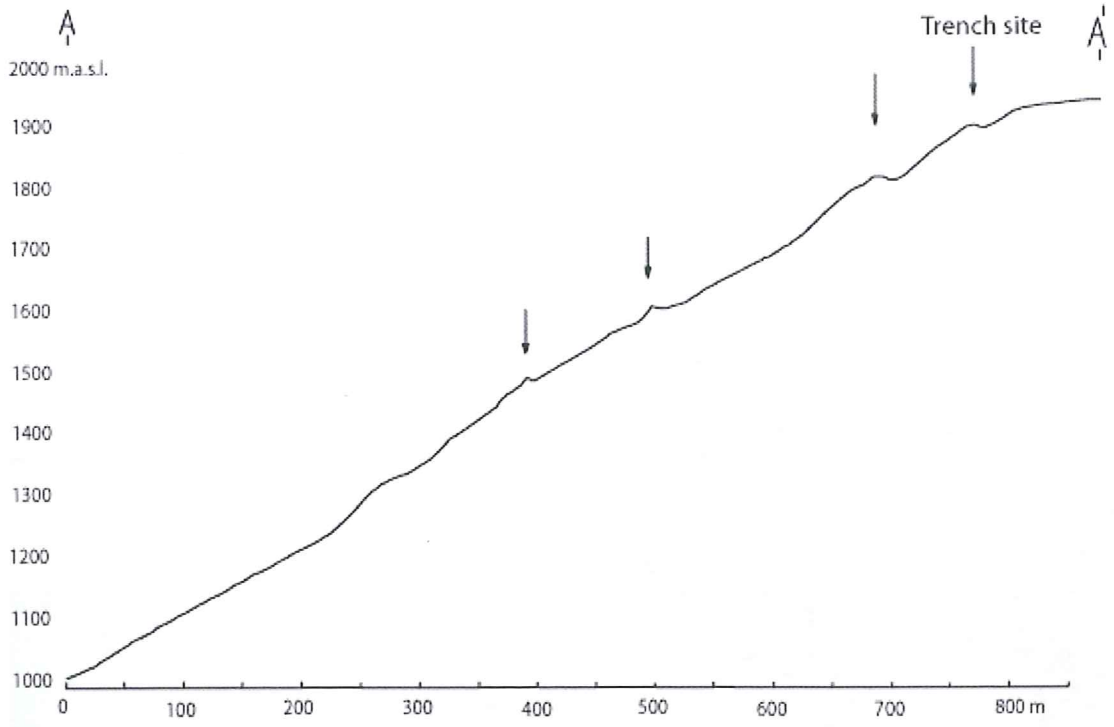

Figure 7. Profile of the slope made from map no 092J055 . Arrows mark the scarps.

4.2 Trench investigation

The trench was made as straight as possible and stopped against a large boulder. Weathered bedrock was found in the bottom of the trench. Three sedimentary units, units 1 – 3, and two types of weathered bedrock were recognised in the trench wall (Fig. 8). Two soils, the modern soil at the surface, and a fossil soil developed in unit 2, were also recorded.

Figure 8. The trench site before trench excavation. The pick marks the trench location. (Photo Magnus Lund.)

4.2.1. Weathered bedrock

Type 1

In the southwestern part, a salmon-pinkish terrigenous clastic detritus unit with a clay matrix and scattered lithic fragments, 5 cm across or smaller, is found at the base of the trench (Fig. 9). Many of the lithic fragments are altered by weathering, some of them heavily. No sedimentary structures can be seen in the layer, which is massive with sporadic clusters of clasts. The clay mineralogy of the matrix was investigated.

X-ray diffraction analysis of the two samples taken between 80 – 120 cm left of 0 (Fig. 9) showed the presence of kaolinite, chlorite, illite, quartz and a mixture of smectite and illite (Fig. 10). A steeply dipping shear zone cuts the layer in the southwest, and the same clastic detritus continues on the other side of the shear plane. The boundary to the weathered bedrock type 2 is a gradual transition zone, approximate 10 cm thick. In the transition zone the two bedrock types are mixed. Weathered bedrock type 1 has its highest position in the southwest and continues downwards beneath weathered bedrock type 2 towards the northeast.

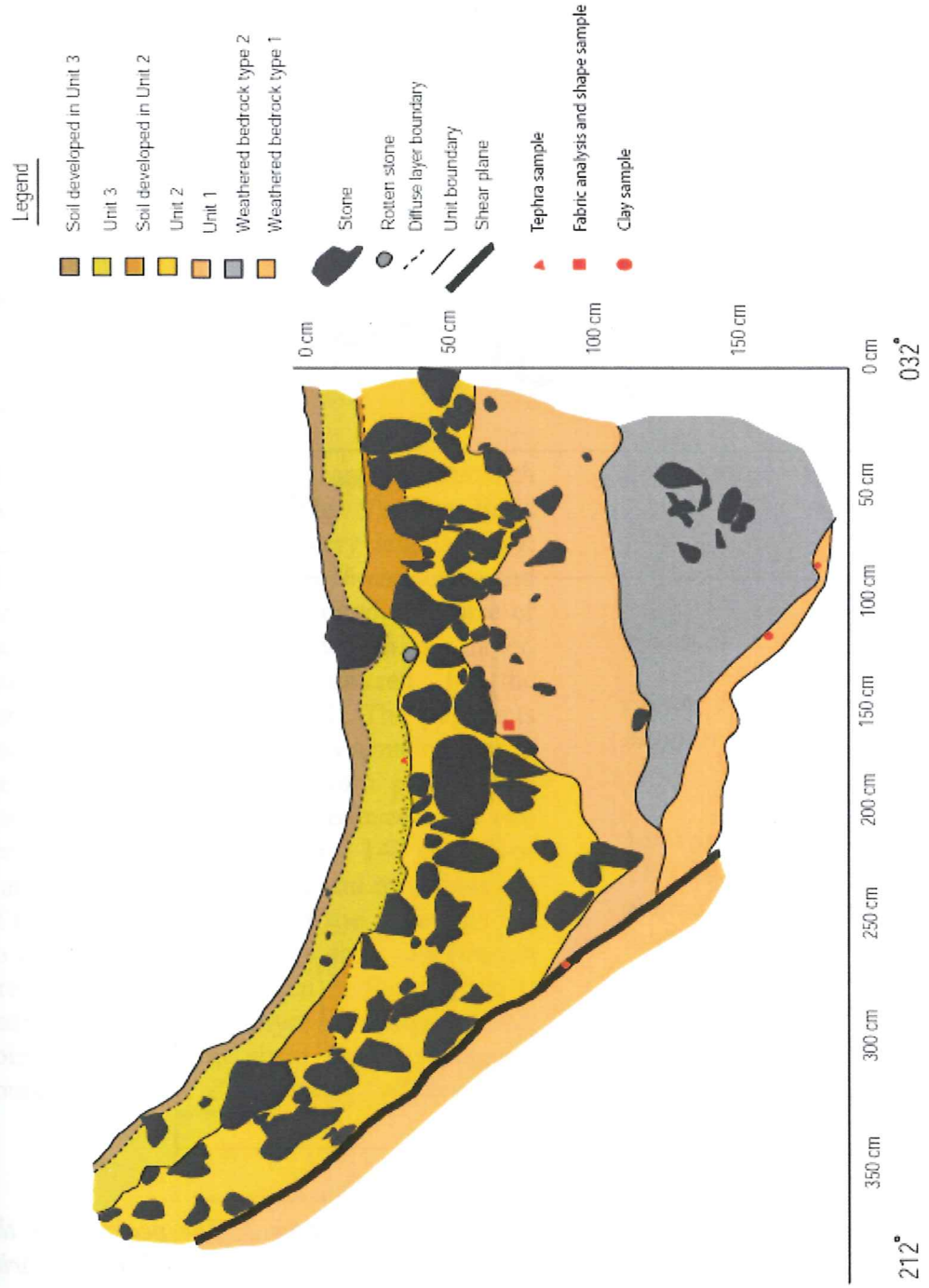

Figure 9. Section chart of sediments in the depression of the investigated anti-slope scarp.

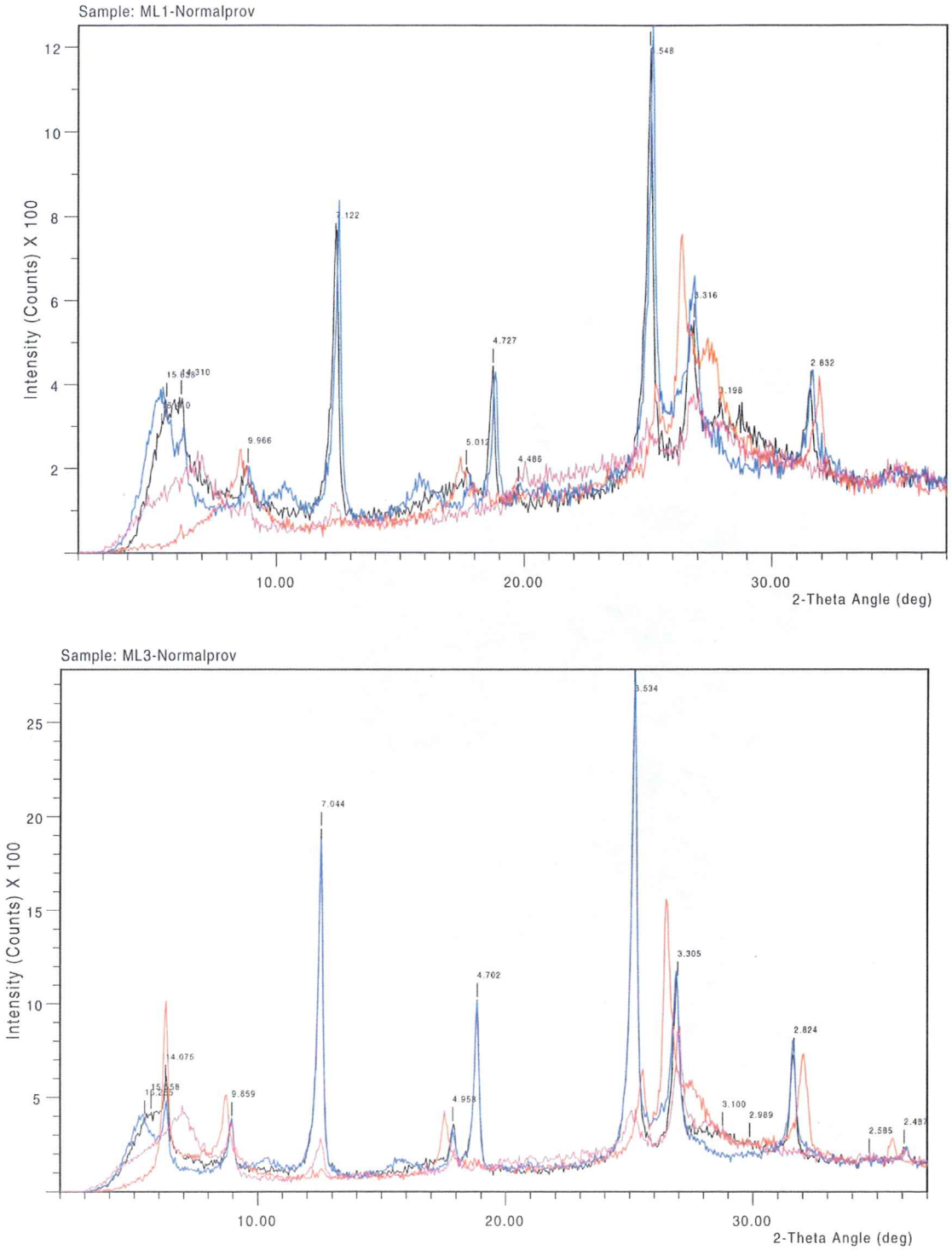

Figure 10. XRD analyses made of the clay in the weathered bedrock type 1. The peaks show the lattice spacing in ångstrom (Å) (Tucker 1988). The peaks of kaolinite are at 7 Å and 3.5 Å; chlorite can be seen at 14 Å, 7 Å, 4.7 Å and 3.5 Å; illite can be seen at 9.8 Å, 4.9 Å, 3.3 Å and 2.4 Å; small peaks of quartz are at 4.2 Å and 3.3 Å. The mixture of smectite and illite have their peaks at 16.4 Å, 8.2 Å, and 5.4 Å.

Interpretation
The layer is interpreted as a regolith. This is based on the highly altered clasts and the matrix lacking sedimentary structures. The clusters of lithic fragments show a lower degree of alteration, while the matrix has new minerals formed by chemical weathering. The boundary towards the shear plane shows rapture while the boundary to bedrock type 2 shows no signs of movement. The lithic fragments are likely to be derived from cores between highly altered criss-crossing fracture zones.

Type 2

This grey layer has a coarse sandy matrix with angular mineral grains (Fig. 9). The lithic fragments are angular or very angular (Fig. 11). The fragments are up to 16 cm across and some of them are heavily altered. The size of the lithic fragments vary within the layer. Larger fragments are clustered in the northeastern part of the trench. The fragments tend to get smaller, generally smaller than 5 cm across, in the southwestern part of this unit. The transitional zone between the two areas is located between 135 – 140 cm left of 0 and is gradational. Matrix and fragments are of the same colour. Within the layer there is no grading or sorting except for a few pinkish streaks, which can be seen in the contact to bedrock type 1. The layer is wedge-shaped, pointing towards the shear plane. The upper boundary to unit 1 is horizontal and very even.

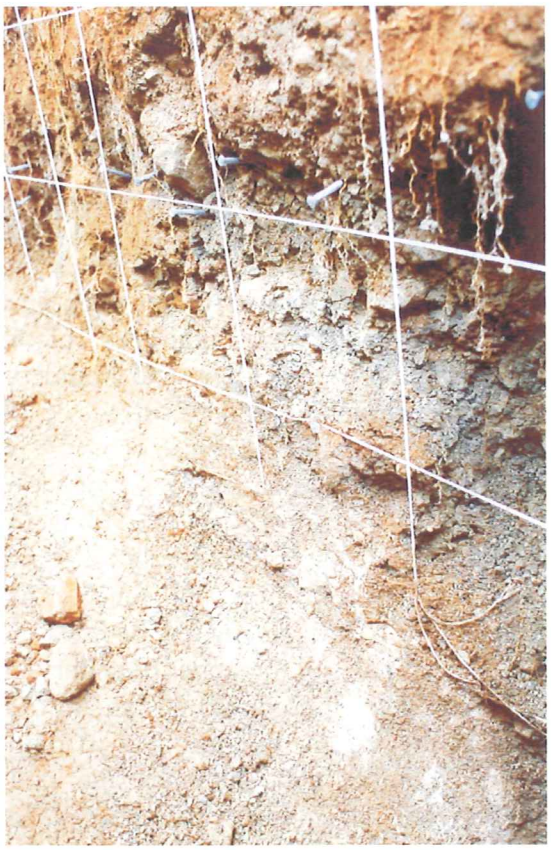

Figure 11. Weathered bedrock type 2. (Photo Magnus Lund.)

Interpretation
This layer is also interpretated as a type of altered bedrock, but different to type 1. The interpretation is based on the observation that all lithic fragments are of the same bedrock type, and that the matrix partly consist of angular mineral grains weathered out of the solid rock. The fractured bedrock is weathered *in situ*. The angular and altered clasts and matrix show no indication of transport. The only structures found within weathered bedrock type 2 are fractures of various size. The boundary to bedrock type 1 (underneath) shows no signs of displacement.

4.2.2. Sediments

Unit 1

This unit differs significantly from the substratum (Fig. 9). It consists of a massive matrix supported diamicton (D(Si-S)mm) with fresh unweathered clasts (Fig. 12). The colour of the matrix is dark brown to greyish. The clasts are either of the same light-grey colour as the bedrock-derived pebbles and boulders found on the surrounding ground surface or of a greenish colour. The greenish colour is characteristic for a sedimentary rock type with a low grade of metamorphism and rounded grains of quartz. This greenish bedrock type does not occur upslope from the trench. The lower boundary to the weathered bedrock is even and horizontal, but the upper boundary is irregular. The layer is thickest, 60 cm, in the mid part of the trench, thinning out in both directions. Towards the southwest the unit thins to less than 25 cm but at the shear plane the unit is extended upwards, following the shear plane for 50 cm. The boundary at the shear plane is sharp with an abrupt lateral transition into weathered bedrock type 1.

The unit is massive without bedding or other sedimentary structures. The texture is homogenous without grading or sorting of the diamict matrix. The matrix consists of sand, gravel as well as silt. Small amounts of clay are also present, but clay content is less than 5%. Sorting is very poor. The unit has sporadically scattered clasts. The largest clasts are of pebble size, up to 10 cm across, and sub-angular to sub-rounded.

The clasts collected at the site for fabric analysis (at 165 cm, depth 75 cm) showed that the clasts are not in a single category, they occur in all four types of shapes (discoid-, equant-, bladed- and rod-shaped) with clustering around the border of the four categories. Clast a-axis was measured to be between 23 and 52 mm long. The fabric-analysis showed an a-axis S1-value of 0,521 with a preferred orientation of the clasts (V1) of 323°/31° (Fig 13).

Figure 12. Unit 1. (Photo Magnus Lund.)

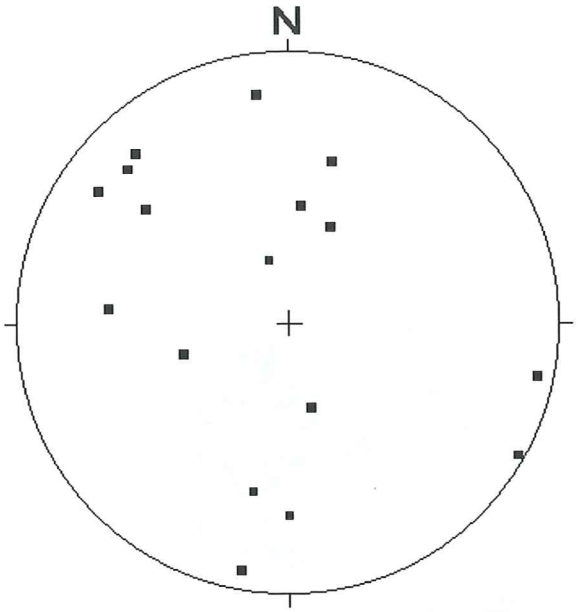

Figure 13. Result of fabric analyses of clast a-axes in unit 1.

Interpretation

Unit 1 is interpreted as primary till deposited at the base of a glacier, even if all criteria for lodgement till are not full-filled (Dreimanis 1989). The interpretation is based on following facts:

1. The unit consists of un-weathered debris differing significantly from the regolith below;
2. The grain size distribution is caracteristic of a diamicton with distinct modes in the silt and gravel ranges which probably represent rock flour produced by abrasion and gravel produced by crushing (Benn and Evans, 1998);
3. The homogeneity of the diamict texture and the massive structure indicate that deposition occurred without changes or interruptions in the sedimentary process;
4. The sub-angular and sub-rounded clasts are signs of intergranular friction and particle abrasion during transport.

The clast fabric does not show a strong preferred orientation, which is expected for a lodgement till (Dreimanis 1989). Postdepositional loading from unit 2 and deformation related to movement along the shear plane, as indicated by the irregular and undulating upper surface, might have disturbed the original clast orientation.

Unit 2

Unit 2 is a heterogeneous, mainly matrix supported, diamicton (D(S)mm), with occasional beds or lenses of clast supported gravel (Gcm) (Fig. 9). The matrix is medium brown, and the clasts are of the same light colour as the clasts on the surrounding ground surface. The unit is approximately 40 cm thick, increasing slightly in thickness towards the shear plane. Between 175 and 275 cm its maximum thickness is about 75 cm. A minimum thickness of 20 cm occurs at 140 cm. The lower boundary in the southwest follows the shear plane, and the boundary towards the shear plane is sharp. The upper boundary to unit 3 is also sharp and partly erosive.

The matrix of the unit is generally a mixture of fine gravel to fine sand with small amounts clay. The matrix is very poorly sorted. The gravel lenses are very loose, and occasionally with an open framework. Towards the northeast the unit tends to be more clast-supported. Boulders and cobbles are angular to sub-angular (Figure 14). The largest clasts are up to 70 cm across. The clasts show no sign of chemical alteration. The percentage of clasts is high, over all about 40 – 60 %, with clasts being larger than 5 cm across. The entire unit is penetrated by rootlets that have caused bioturbation, which has destroyed any stratification or structures (Fig. 14). No fabric analysis was made, but clasts close to the shear plane show a clear orientation parallel to the plane.

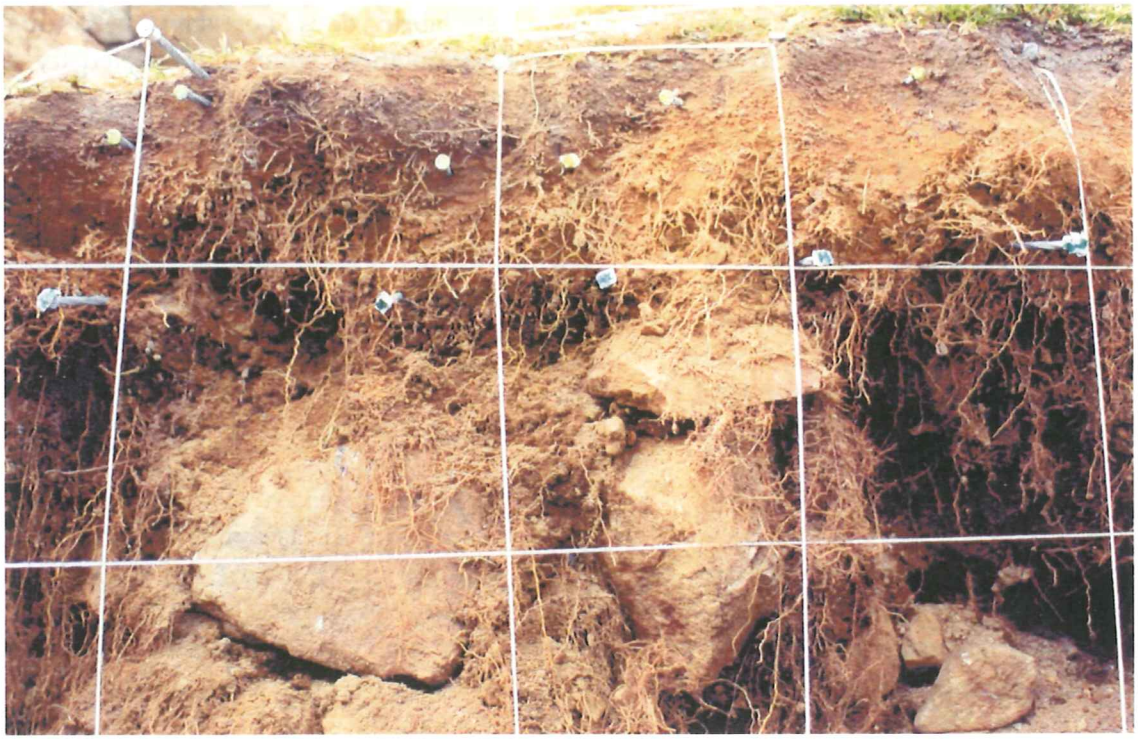

Figure 14. Unit 2 and 3. (Photo Magnus Lund.)

Two dark brown pockets, rich in humus, occur in the uppermost part of the unit. Their upper boundary is sharp and coincides with the upper boundary of the unit. Twenty cm down, the pockets have a diffuse lower transition into the medium brown lower part of the unit. The transition is hard to follow, due to the large number of cobbles and boulders. A shallow erosive channel separates the two pockets.

Interpretation

Unit 2 is interpreted as a colluvium. Gravity-driven mass processes are indicated by the heterogeneous composition of the matrix, the loose character and the high content of angular boulders. A combination of gravitational processes is suggested, and the unit is interpreted as a mixture of fall/slide deposits and flow/creep deposits.

The bouldery, coarse-grained and loose deposits, partly with open frame-work, are interpreted as fall and slide deposits. The angular clasts are of the same rock type as formed in the local hill slope, and the boulders show no sign of glacial or fluvial transport. The present gravity-driven processes in the steep slope are considered an analogy to the formation of the unit, and the similarity to the ongoing accumulation of boulders caught in the shallow depression inside the scarp is striking. Because the bedrock close to the shear plane in the south is weathered the source of the unweathered clasts is most likely lies in the steep hill side to the north. Lenses or layers with a more fine-grained diamict composition indicates cohesive debris flows, either as slow creep of more rapid solifluction of mud flows. The source of the cohesive flows may be from either the sharp ridge or the hill slope.

The darker, uppermost part of the unit is interpreted as a fossil soil, coloured by humus. The discontinuity of the soil was caused by fluvial erosion before deposition of unit 3. The palaeosol indicates that the upper

surface of unit 2 has constituted a ground surface and that the slope probably was more stable during a prolonged period of time.

Unit 3

The unit is 20 cm thick and consists of 2 cm of coarse to medium sand overlain by finer sand (fSm – mSm) (Fig. 9). Smaller amounts of clay, less then 5%, occur within the unit. The lower contact is erosive, with a shallow depression cut into the palaeosoil surface of unit 2 between 100 and 250 cm. The upper surface is smooth. The southern part of the layer is bent in a monoclinal flexure, while the central and northeastern parts are approximately horizontal. The colour is rusty to grey. The greyer parts are immediately below the vegetation, and the rest of the uppermost 5 cm are dark brown to black with a high amount of humus and abundance of fine roots.

The coarse sand at the base of the unit shows diffuse planar parallel lamination. The grains consist of tephra and quartz that are rounded to well rounded. A sample of the sand was studied in a microscope, and the glass content in the sand was found to be high, but the proportions were difficult to determine. The finer sand in the upper part is massive. Outsized clasts, up to 20 cm in diameter, are scattered throughout the unit. The clasts are of the same type as the large clasts on the ground and generally angular, but with a uniaxial shape. With one exception they are all unweathered. A highly altered clast was found at 125 cm in the lower part of the unit (Fig. 14).

Interpretation

The grain size and the stratification in the lower parts suggest transport and deposition by fluvial flow (Nichols, 1999). The stream was small and shallow, and deposition was preceded by fluvial erosion. The finer sand indicates very slow through-flow and a transition to ponded water. Originally the layer must have been horizontal, showing that the monoclinal bending occurred after deposition.

The admixture of tephra and non-volcanic grains indicates reworking of pyroclastic fallout deposits from the surrounding slopes.

The presence of roots in the uppermost part, together with the weak zones of geochemical leaching and accumulation, indicate the development of a modern soil.

4.2.3. The shear-plane

Weathered bedrock of type 1 was found from the bottom to the top of the trench at the southwestern side of the shear zone and at the base of the trench on the northern side (Fig. 9). The boundary to overlying sediments is very sharp in the trench, and so is the transition to weathered bedrock at the other side of the shear zone. The four sediment units in the hanging wall are bent in a monocline close to the shear zone. The strike and dip of the shear-plane varies between 320°/41° (lower parts) and 321°/46° (measured higher up). Slickenlines found at a depth of 80 – 100 cm showed a deviation of 19° towards the east from the slope direction. The colour of the clay is greyish (Fig. 15).

The grain size composition of the clay in the shear zone is finer in the lower parts compaired to the contact to unit 1 and 2. This gives the impression that the diamict debris was smeared out and mixed with the clay in the shear zone.

Figure 15. Picture of the shear-plane with the shovel as scale. (Photo Magnus Lund.)

A sample for XRD analysis was taken in the lower parts of the shear-plane at a depth of 80 – 100 cm. The XRD results show the presence of kaolinite, chlorite, illite, quartz and a mixture of smectite and illite (Fig. 16). The movement at the shear plane is an upthrowing of the footwall, the slickenlines show a slight movement sideways. The sediments are disturbed and have a monoclinal bending in the southwestern parts of the trench.

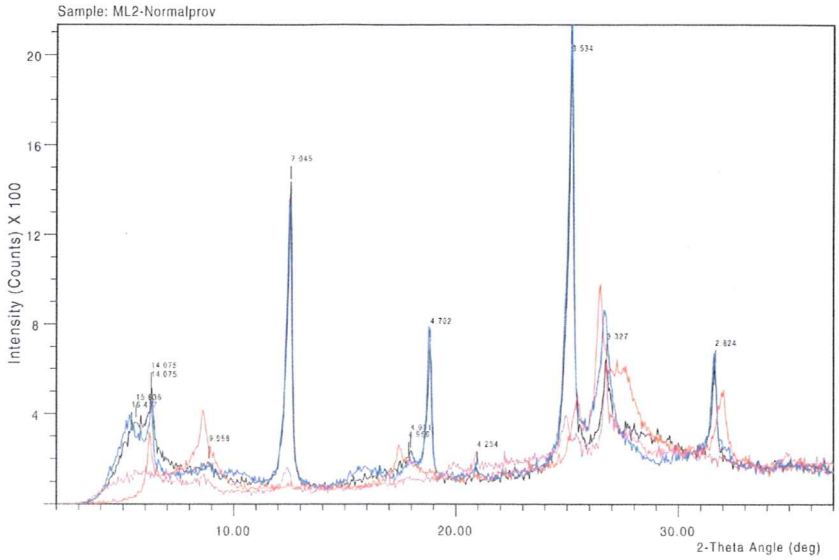

Figure 16. Results of XRD analyses made on the clay in the shear zone. The peaks show the lattice spacing in ångstrom (Å) (Tucker 1988). The different peaks of kaolinite are at 7 Å and 3.5 Å; chlorite peaks are shown at 14 Å, 7 Å, 4.7 Å and 3.5 Å; illite have their peaks at 9.8 Å, 4.9 Å, 3.3 Å and 2.4 Å; the presence of quartz are confirmed by the peaks at 4.2 Å and 3.3 Å. The mixture of smectite and illite have their peaks 16.4 Å, 8.2 Å, and 5.4 Å.

4.3. Ground penetrating radar

GPR radargrams were used for the interpretation of subsurface structures and to interpret boundaries between weathered and solid rock. The cross-sectional profile from the radargram records run parallel to the trench and perpendicular to the anti-slope scarp (Fig. 17).

No distinct structures are seen on the radargrams, and the data are not easily interpreted. Irregularities in the record from the footwall might be interpreted as thrust-planes parallel to the shear-zone recognised in the trench. If this is the case, they represent a series of normal faults descending towards the small depression inside the ridge and directed towards the general upslope direction.

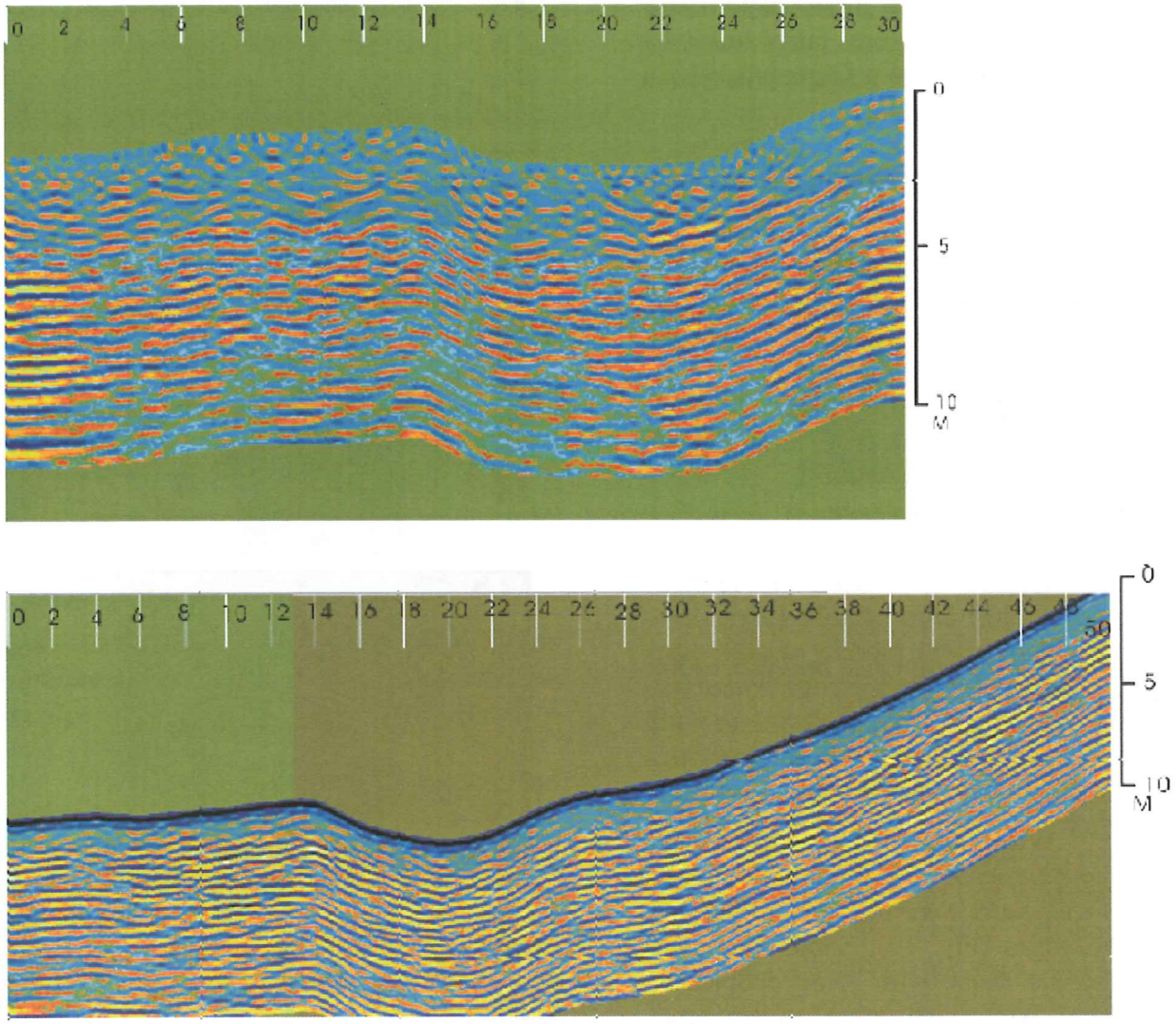

Figure 17. GPR image that was taken parallel to the trench. File no 1538 (above) is 30 m long and 1541 (below) is 50 m long.

4.4. Dating by tephra

Sand with tephra, found in the lower part of unit 3, was sampled in order to correlate the tephra to known tephra horizons in the mountain area. The sampled sand has a dark, warm brown colour, and the grain-size analysis shows that it is a moderately sorted medium sand (Fig. 18), with only small amounts of coarser and finer sand. The individual tephra grains are fairly easy to crush between a finger and a fingernail, which leaves a fine powder.

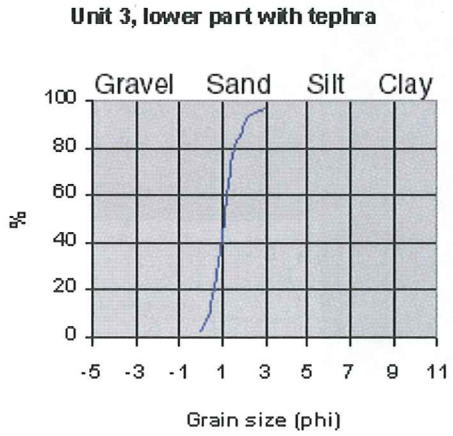

Figure 18. Result of grain size analysis of the lower part of unit 3 with tephra.

When inspected in a polarizing microscope fragments of glass could be seen. The glass fragments were transparent and had very sharp edges (Fig. 19). Some fragments had a spherical shape with some bubbles in them. There were also other minerogenic particles that were visible with crossed polars, but the volcanic content exceeded the non-volcanic detritus.

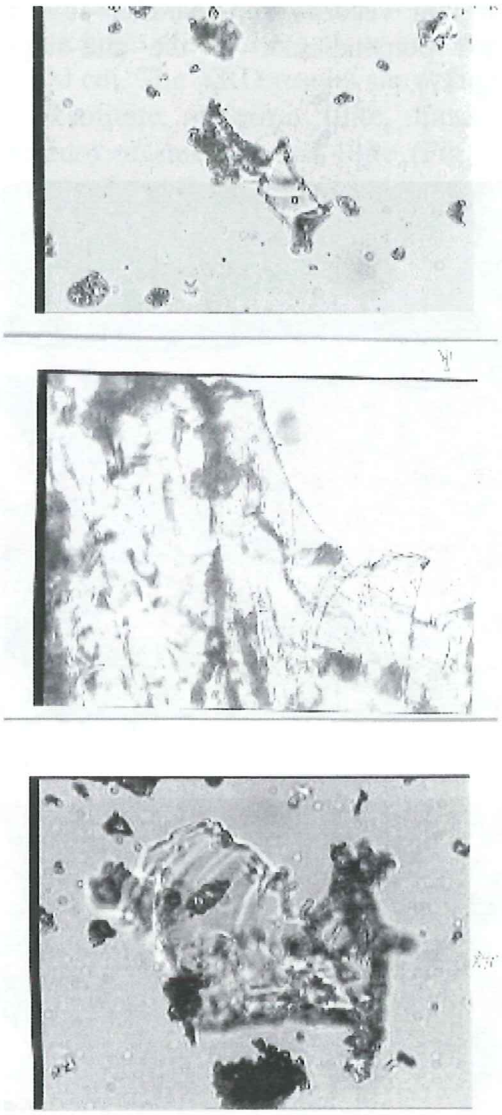

Figure 19. Crushed tephra seen in a microscope at x40 magnification. (Photo Magnus Lund.)

Several volcanic eruptions have affected the mountain area, but only two tephra horizons are known from the investigated site, the Bridge River Tephra and the Mazama Tephra (Fig 20). The Bridge River Tephra have an index of 1,499 – 1,503, and the Mazama Tephra has an index of 1,505 and higher. The two types of tephra cannot be separated by the index.

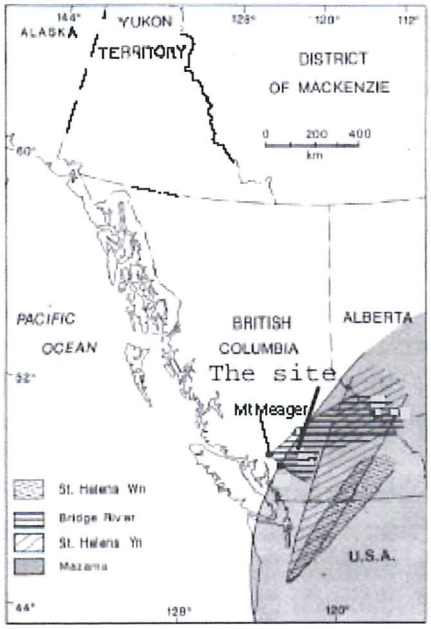

Clague et al 1995.

Figure 20. Distribution of tephra fall-out from eruptions that may have affected the investigated area.

The tephra can, however, be identified by grain size. The Mazama Tephra can be ruled out because of the long distance to the eruption site, which is situated in Crater Lake, former Mt Mazama. The eruption site is located 800 km from the investigated site in southern Oregon, U.S.A. (Clague 1989). Only fine-grained ash from this eruption is expected at the investigated site. The eruption site of Bridge River Tephra is situated 15 km away, and medium sand particles can be expected in the area.

4.5. Interpretation of the depositional and deformational history

The sediments in the catchment inside the scarp at Handcar Peak are underlain by weathered bedrock containing clay minerals. Clay minerals are generally used as indicators of the degree and character of weathering. The different types of clay minerals from the investigated samples can be the product of soil forming processes, but may also be formed by hydrothermal alteration at temperatures between 150° and 190° (Table 1).

Andesitic and rhyolitic lava flows	
Smectite	60-190°C
Kaolinite	110-210°C
Illite	100-150°C
Chlorite	150-310°C

Table 1. Temperatures required for clay forming (Martini et al. 1992).

Independent of the genesis, the weathered bedrock indicates the timing of shear-plane activity. It is not likely that weathered bedrock could resist erosion in the steep hillside without a protecting position in a depression surrounded by hard rock. The up-thrown, weathered bedrock on the southwestern side continues most likely into more firm bedrock separated by further shear-planes, as indicated by the GPR radargram.

The till on top of the altered bedrock is most likely of late Wisconsinan age and belongs to the Frasier glaciation. Tills from older glaciations are very rarely found in the mountain area. The depression in the slope is very shallow, and there is only one till in the investigated sequence.

After deglaciation the site existed as a small inclined platform in the steep slope of the u-shaped valley. Slope

processes started in the exposed hillside, and the step in the slope caught rolling out-runners and debris from the slope processes. Gravity displacements are particularly common in unstable, over-steepened slopes exposed by glacier retreat (Ritter *et al.* 1995).

The buried soil on top of unit 2 indicates a period of increased slope stability at the site. The mixture of tephra and non-volcanic clasts in the sand of unit 3 implies reworking by slope-wash from the hillside. This might be the result of increasing humidity or a change within catchment. This change was preceded by the volcanic activity of the Bridge River eruption dated to 2.4 ka BP.

During sedimentation of unit 3 a cobble of weathered bedrock fell into the small basin. It is probable that the clast came from weathered bedrock related to the shear zone, and that the formation of the depression was caused by activation of the fault. Sedimentation of unit 3 was succeeded by activity along the shear plane in the southwestern part of the trench. This resulted in formation of the scarp, deformation of the sediments in the section in a monoclinal bend, and the present morphology of the depression.

5. Discussion

One theory for the formation of anti-slope scarps in the area can immediately be excluded based on present results. This is the theory that explains the scarp and the depression as formed by erosion. The section in the trench clearly shows that faulting and bending of strata govern the topography. But how and why did the scarp arise? Was it a slow, gradual displacement or a rapid disruption? What triggered the thrusting?

The formation of the anti-slope scarp at Handcar Peak seems to be a very young occurrence. The scarp is related to the shear-plane in the trench, and movements along the plane occurred after deposition of the uppermost unit, which in turn is younger than the Bridge River Tephra dated to 2.4 ka BP (Clague *et al.* 1995). The preservation of saprolitic bedrock suggest that the depression exsisted already prior to the Frasier glaciation. This indicates that movements along parallel shear-planes have occurred at repeated times.

The steeply dipping shear-plane in the trench continues into the bedrock and is not only related to surface processes. The northwest – southeast trend of the thrust-plane and the anti-slope scarp coincides with major joint-sets and faults in the area (Fig. 2) formed during post-Early Cretaceous shearing (Friedman *et al.* 1995). The displacement was most likely a reactivation along a pre-existing zone of weakness in the bedrock.

The fault and the monoclinal bend represent both brittle and ductile deformation. Ductile warping of sediments has been interpreted as evidence of gradual movement (Thompson *et al.* 1997), and warping is also common in other trenches where slow displacements of probable gravitational origin have occurred (McCalpin *et al.* 1995). Brittle displacements would more likely occur during catastrophic events. Colluvium is commonly deposited at scarps formed during earthquakes (McCalpin *et al.* 1994). Evidence of extensive rock fall or other slope processes related to displacements is not found in the section. The colluvium in the trench was deposited long before the deformation event. Large boulders on the surface do, however, occur further to the north in the depression (Fig. 4), and a catastrophic disruption cannot be ruled out.

Two theories for the triggering mechanism have been suggested, one is gravitational failure of the mountain slope, the other neo-tectonics. Gravitational spreading of slopes is supposed to occur during or after glacial retreat (Bovis 1982, 1990; McCalpin *et al.* 1995). This process is induced by the ice decay, which reduces pressure on the hillside, making the mountain expand under the

pressure of its own weight. This is a process that may take thousands of years, and results in subsidence of the mountain in the direction of the pressure release after decay of the ice sheet (Beck 1967). The pressure release model cannot directly be related to the anti-slope scarps in the hillside southeast of Handcar Peak, as the scarps are not perpendicular to the slope. This would be expected from gravitational spreading acting in a steep slope. Moreover, the timing of scarp formation is not connected to the decay of the ice sheet. Other types of gravitational failure are not consistent with the fact that the scarps are facing the hillside.

Neotectonics related to isostatic rebound after Frasier glaciation has been proposed as triggering mechanisms for the formation of scarps (Thompson *et al.* 1997; Beck 1967; McCalpin *et al.* 1995). The isostatic rebound was more rapid during and immediately after deglaciation and most isostatic recovery was completed 6 – 9 ka BP (Clague *et al.* 1982). Disruption and deformation of sediments and bedrock at Handcar Peak took place at a much later time.

Neotectonics related to activity along the edge of the North American lithosphere plate is also a possible trigger. The area is a tectonic part of Canada. Two major earthquakes have been recorded during pre-historic time. One occurred about 1700 years ago, with a magnitude of 8 (Clague *et al.* 1998). On average, there is one earthquake of magnitude 6 or larger every 10 to 15 years in southern British Columbia (Clague *et al.* 1998). Several faults are located in the Coast Mountains, parallel to the scarps and to the major joint sets and faults in the investigated area (Friedman *et al.* 1995). Measurements on small earthquakes in southern British Columbia also show that the maximum rate of earth crust elongation in the area is directly east – northeast, perpendicular to the anti-slope scarps and the normal fault at Handcar Peak (Thompson *et al.* 1997).

Both the theory of gravitational spreading related to ice-sheet deglaciation, and the theory of neo-tectonics related to plate boundary, were explored through searching for literature on anti-slope scarps from the Caledonian Mountain Range area in Scandinavia. The Scandinavian mountains have been affected by the Weichselian Ice Sheet, but are situated in a stable crust area. Descriptions of features similar to the scarps in the Coast Mountains were not found. Similar features are, however, found in the Alps and in the Carpathian Mountains (Zischinsky 1969; Jahn 1964), which are tectonically active areas.

6. Conclusions

The investigated trench was excavated through an anti-slope scarp situated in an area with more than 60 anti-slope scarps with a consistent northwest – southeast trend. This direction coincides with failure planes in the bedrock, and the shear zone exposed in the trench shows normal faulting related to the scarp. A tectonic origin is suggested for the formation of the scarp.

The sediment infilling of the small depression inside the up-slope facing scarp consist of fluvial sediments, rock fall and gravity flow deposits, and a basal till deposited on top of deeply weathered bedrock. The preservation of weathered bedrock and a monoclinal bend of the strata suggest repeated events of displacements, both prior to and after Frasier glaciation.

The disruption of the crust was not related to unloading after deglaciation. This is shown by the presence of reworked Bridge River Tephra in the fluvial sediments, which dates the normal fault and the bending of strata to the late Holocene, after 2.4 ka BP. The most probable triggering mechanism for the formation of the scarp at Handcar Peak is an earthquake related to plate tectonics.

Acknowledgements

For financial support I would like to thank Lund University. I also would like to thank Barbara Wohlfarth for making me take the step over the Atlantic Ocean. Thank you John Clague for letting me in on this project and all the help you have provided. Thank you Steve Evans for the slope measurements and Joseph Chow for the GPR image and for all the other help I got in the field.

Thank you Lena Adrielsson, for taking your time to supervise me. I am also grateful for the help I got from Anders Lindh to analyse the rock samples. Thank you Zoltan Solyom for helping me with my clay samples, and Anders Ahlberg and Ingela Olsson for giving me advice about how to interprete the clay mineralogy data.

Finally, I would like to say thanks to Mats Rundgren for reading and highlighting my errors and Fredrik Quist for checking my English spelling and my lousy grammar.

References

Literature

Beck, A.C. (1968). Gravity faulting as a mechanism of topographic adjustment. *N. Z. J. Geol. Geophys.* Vol. 11, pp 191 – 199.

Bell, J. S., Eisbacher, G. H., (1996). Neotectonic stress orientation indicators in southwestern British Columbia. In: *Current Research 1996-A*: Geological Survey of Canada, Ottawa, Ontario, pp 143 – 154.

Benn, D. I. and Evans D. J. A. (1998). *Glaciers and Glaciation*. Bath, Great Britain.

Bovis, M. J. (1982). Uphill-facing (antislope) scarps in the Coast Mountains, southwest British Columbia. *Geological Society of America Bulletin,* Vol. 93, pp 804 – 812.

Bovis, M. J. (1990). Rock-slope deformation at Affliction Creek, southern Coast Mountains, British Columbia. *Canadian Journal of Earth Sciences*, Vol. 27, pp 243 – 254.

Bovis, M. J., and Evans, S. G. (1995). Rock slope movements along the Mount Currie "fault scarp," southern Coast Mountains, British Columbia. *Canadian Journal of Earth Sciences*, Vol. 32, pp 2015 – 2020.

Clague, J. J., Evans, S.G., Rampton, V.N. and Woodsworth, G.J. (1995). Improved age estimates for the White River and Bridge River tephras, western Canada. *Canadian Journal of Earth Sciences. Vol. 32, No. 8*, Pp 1172 – 1179.

Clague, John J., (1989). Geological Survey of Canada. Geology of Canada; no. 1. *Quaternary geology of Canada and Greenland*. Pp 17 – 37. Edited by R.J. Fulton. Ottawa, Canada

Clague, John J., Bobrowsky, P. T., Hutchinson, I., Mathewes, R. W., (1998a). Geological evidence for past large earthquakes in southwest British Columbia. *Geological Survey of Canada.* Pp 217 – 224.

Clague, John J., Naesgaard, E., Mathewes, R. W., (1998b). Geological evidence for prehistoric earthquakes. *Geology and Natural Hazards of the Fraiser River Delta, British Columbia. Geological Survey of Canada, Bulletin 525.* Pp177 – 194.

Dreimanis, A. (1989). Tills: Their genetic terminology and classification. In: *Genetic classification of glacigenic deposits*. Edited by: Goldthwait, R.P. and Matsch, C.L. pp 17 – 84.

Evans, S. G. (1987). Surface displacements and massive toppling on the northeast ridge of Mount Currie, British Columbia. In: *Current Research, part A*. Geological Survey of Canada, Paper 87-1A, pp 181 – 189.

Eyles, F., Eyles, C. H., Miall, A. D., (1983). Lithofacies types and vertical profile models; an alternative approach to the description and environmental interpretation of glacial diamict and diamictite sequences. *Sedimentology*, vol. 30, pp 393 – 410.

Folk, R. L., and Ward, W., (1957). Brazos River bar: a study in the significance of grain size parametres. *Journal of Sedimentary Petrology.* Vol. 27. Pp 3 – 26.

Friedman, R. M. and Armstrong, R. L., (1995). Jurassic and Cretaceous geochronology of the Coast Belt, British Columbia, 49° to 51° N. In: *Miller, D.M. and Busby, C., Jurassic Magnetism and Tectonics of the Northern American Cordillera: Boulder, Colorado.* Geological Society of America Special Paper 299.

Hardy, R., Tucker, M., (1988) X-ray powder differaction of sediments. In: *Technics in Sedimentology*. (Editor: Tucker, M.) *Blackwell Scientific Publications*, Oxford, London. Pp. 191 – 228.

Jahn, A. (1964). Slopes morphological features resulting from gravitation. *Zeitschrift fur Geomorphologie, Suppl.* 5, pp 59 – 72.

Mark, D. M. (1973). Analysis of axial orientation data, including till fabrics. *Geological Society of America Bulletin.* Vol. 84, pp 1369 – 1374.

Martini, I.P., Chesworth, W. (1992). *Developments in Earth Surface Processes 2, Weathering, Soils & Palesols*. New York.

McCalpin, J. P., and Irvine, J. R. (1995). Sackungen at the Aspen Highlands Ski Area, Pitkin County, Colorado. *Environmental and Engineering Geosciences*, Vol. 1, No. 3, Fall, pp 277 – 290.

McCalpin, J. P. (1996). *Paleoseismology*. San Diego, USA.

Nichols, Gary (1999). *Sedimentology and stratigraphy*. University Press, Cambridge, Great Britain.

Quaternaria. (1995). *Kompendium I jordartsanalys -laboratorieanvisningar*. Stockholms Universitet. Ser.B, No 1. Stockholm, Sweden.

Pettijohn, F.J. (1975). *Sedimentary Rocks*, pp 628, Harper & Row, New York.

Ritter, D. F., Kochel, R. C., Miller, J. R. (1995). Processes in geomorphology. Third edition. Dubuque, USA.

Ryder, J. M., Fulton, R. J., Clague, J. J. (1991). The Cordilleran Ice Sheet and the Glacial Geomorphology of Southern and Central British Columbia. *Géographie physique et Quaternaire*, vol. 45, no. 3, pp. 365 – 377.

Tabor, R. W. (1971). Origin of Ridge-Top Depressions by Large-Scale Creep in the Olympic Mountains, Washington. *Geological Society of America Bulletin*, Vol 70, pp 1811 – 1822.

Thompson, S.C., Clague, J.J., Evans, S.G., (1997). Holocene Activity of the Mt. Currie Scarp, Coast Mountains, British Columbia, and Implications for its Origin. *Environmental and Engineering Geosciences*, Vol III, No. 3, Fall, pp 329 – 348.

Tucker, M. (1981). Sedimentary Petrology, an introduction. *Blackwell Scientific Publications*. London, Great Britain.

Zischinsky, U. (1969). Uber sackungen. *Rockmechanics.* Vol. 1/1.

Maps

Province of British Columbia (1995). *Ministry of Environment, Lands Parks Surveys and Resource Mapping Branch*. Sheet number according to British Columbia Geographic System 92J.055. Scale 1:20 000. Declination 20° 52' west. Universal Transverse Mercator Projection.

North Creek, Lillooet Land District, British Columbia (1976). *Surveys and mapping branch, Department of Energy, Mines and Resources*. Series A721, map 92J/11, 1st edition. Scale 1:50000. Declination 23° 53'. Transverse Mercator Projection

WebPages

http://www3.calle.com/info.cgi?lat=50.3167&long=-122.8167&name=Pemberton&cty=Canada&alt=2014
Map over Pemberton area.
Download date: 2001-10-21.

http://geography.about.com/gi/dynamic/offsite.htm?site=http://toporama.cits.rncan.gc.ca/
Map over Handcar area.
Download date: 2002-03-05.

Tidigare skrifter i serien "Examensarbeten i Geologi vid Lunds Universitet":

89. Antonsson, Christina, 1997: Inventering, hydrologisk klassificering samt bedömning av hydrogeologisk påverkan av våtmarksområden i samband med järnvägstunnelbyggnation genom Hallandsåsen, NV Skåne.
90. Nordborg, Fredrik, 1997: Granens mark-påverkan - en studie av markkemi, jordmånsbildning och lermineralogi i gran- och lövskogsbestånd i södra Småland.
91. Dobos, Felicia, 1997: Pollen-stratigraphic position of the last Baltic Ice Lake drainage.
92. Nilsson, Johan, 1997: The Brennvinsfjorden Group of southern Botniahalvøya, Nordaustlandet, Svalbard - structure, stratigraphy and depositional environment.
93. Tagesson, Esbjörn, 1998: Hydrogeologisk studie av grundvattnets kloridhalter på östra Listerlandet, Blekinge.
94. Eriksson, Saskia, 1998: Morängenetiska undersökningar i klintar vid Greifswalder Boddens södra kust, NÖ Tyskland.
95. Lindgren, Johan, 1998: Early Campanian mosasaurs (Reptilia; Mosasauridae) from the Kristianstad Basin, southern Sweden.
96. Ahnesjö, Jonas, B., 1998: Lower Ordovician conodonts from Köpings klint, central Öland, and the feeding apparatuses of *Oistodus lanceolatus* Pander and *Acodus deltatus* Lindström.
97. Rehnström, Emma, 1998: Tectonic stratigraphy and structural geology of the Ålkatj-Tielma massif, northern Swedish Caledonides.
98. Modin, Anna-Karin, 1998: Distributionen av kadmium i moränmark kring St. Olof, SÖ Skåne.
99. Stockfors, Martin, 1998: High-resolution methods for study of carbonate rock: a tool for correlating the sedimentary record.
100. Zillén, Lovisa, 1998: Late Holocene dune activity at Sandhammaren, southern Sweden -chronology and the role of climate, vegetation, and human impact.
101. Bernhard, Maria, 1998: En paleoekologisk -paleohydrologisk undersökning av våtmarks-komplexet Rolands hav, Blekinge.
102. Carlemalm,Gunnar, 1999: En glacialgeologisk studie av morän och moränfyllda sprickor i underliggande sandursediment, Örsjö, Skåne.
103. Blomstrand, Malou, 1999: 1992-1998 Seismicity and Deformation at Mt. Eyjafjalla-jökull volcano,South Iceland.
104. Dahlqvist, Peter, 1999: A Lower Silurian (Llandoverian) halysitid fauna from the Berge Limestone Formation, Norderön, Jämtland, central Sweden.
105. Svensson, Magnus A., 1999: Phosphatized echinoderm remains from upper Lower Ordovician strata of northern Öland, Sweden - preservation, taxonomy and evolution.
106. Bengtsson, Anders, 1999: Trilobites and bradoriid arthropods from the Middle and Upper Cambrian at Gudhem in Västergötland, Sweden.
107. Persson, Christian, 1999: Silurian graptolites from Bohemia, Czech Republic.
108. Jacobson, Mattias, 1999: Five new cephalopod species from the Silurian of Gotland.
109. Augustsson, Carita, 1999: Lapillituff som bevis för underjurassisk vulkanism av strombolikaraktär i Skåne.
110. Jensen, Sigfinn J., 1999: En silurisk transgressiv karbonatlagerföljd vid S:t Olofsholms stenbrott, Gotland.
111. Lund, Mats G., 1999: En strukturgeologisk modell för berggrunden i Sarvesvagge - Luottalako-området, Sareks Nationalpark, Lappland.
112. Magnusson, Jakob, 1999: Exploration of submarine fans along the Coffee Soil Fault in the Danish Central Graben.
113. Wickström, Jenny, 1999: Conodont biostratigraphy in Volkhovian sediments from the Mäekalda section, north-central Estonia.
114. Sjögren, Per, 1999: Utmarkens vegetationsutveckling vid Ire i Blekinge, från forntid till nutid - en pollenanalytisk studie.
115. Sälgeback, Jenny, 1999: Trace fossils from the Permian of western Dronning Maud Land, Antarctica.
116. Söderlund, Pia, 1999: Från gabbro till granat-amfibolit. En studie av metamorfos i Åker-metabasiten väster om Protoginzonen, Småland.
117. Jönsson, Karl-Magnus, 2000: Sedimentologiska och litostratigrafiska undersökningar i södra Malmös kvartära avlagringar, södra Sverige.
118. Romberg, Ewa, 2000: En sediment- och biostratigrafisk undersökning av den tidigare Littorina-lagunen vid Barsebäck, SV Skåne, med beskrivning av en Preboreal klimat-oscillation.
119. Bergman, Jonas, 2000: Skogshistoria i Söderåsens nationalpark. En pollenanalytisk studie i Söderåsens nationalpark, Skåne.
120. Lindahl, Anna, 2000: En paleoekologisk och paleohydrologisk studie av fuktängar i Bräkneåns dalgång, Bräkne-Hoby, Blekinge.
121. Eneroth, Erik, 2000: En paleomagnetisk detaljstudie av Sarekgångsvärmen.
122. Terfelt, Fredrik, 2000: Upper Cambrian trilobite

faunas and biostratigraphy at Kakeled on Kinnekulle, Västergötland, Sweden.

123. Sundberg, Sven Birger, 2000: Vattenrening genom komplexbildning mellan järn och humusämnen - en litteraturstudie med försök.
124. Sundberg, Sven Birger, 2000: Sedimentationsprocesser och avlagringsmiljö för en kantrygg kring platåleran vid Rydsgårds gods i backlandskapet söder om Romeleåsen, Skåne.
125. Kjöllerström, Anders, 2000: En geokemisk studie av bergartsvariationen på Bullberget i västra Dalarna.
126. Cinthio, Kajsa, 2000: Senglacial och tidigholocen etablering och expansion av lövträd på en lokal i nordvästra Rumänien.
127. Lamme, Sara, 2000: Klimat- och miljöförändringar under holocen i Sylarnaområdet, södra svenska Skanderna, baserat på analys av makrofossil och klyvöppningar.
128. Jönsson, Charlotte, 2000: Geologisk och hydrogeologisk modellering av området mellan Bjuv och Söderåsen, nordvästra Skåne.
129. Kleman, Johan, 2001: Utvärdering av den underkambriska litostratigrafin på Österlen, södra Sverige.
130. Sundler, Malin, 2001: En jämförande studie mellan uppmätt och MACRO-simulerad pesticidutlakning på ett odlingsfält i Skåne.
131. Grönholm, Anna, 2001: Högtrycksmetabasiter i den södra delen av Mylonitzonen: fältgeologi, petrografi och metamorf utveckling.
132. Ekdahl, Magnus, 2001: En studie av Källsjögranitens deformationsmönster och kinematiska indikatorer inom Ullaredszonen.
133. Axheimer, Niklas, 2001: Middle Cambrian trilobites and biostratigraphy of the Almbacken drill core, Scania, Sweden.
134. Lindén, Mattias, 2001: Proglacial deformation of glaciofluvial sediments during the Pomeranian deglaciation in the Neubrandenburg area, NE Germany.
135. Warnhag, Jon, 2001: A geochemical study of the zoned Pan-African Mon Repos intrusion, Central Namibia.
136. Lundmark, Mattias, 2001: Zirkonstudie av Norra Hortens bergarter, SV Sverige.
137. Gunnarson, Rebecka, 2001: Sedimentologisk undersökning av en moränskärning i en djupvittrad sprickdal på Romeleåsen, Skåne.
138. Karlsson, Christine, 2001: Diagenetic and petrophysical properties of deeply versus moderately buried Cambrian sandstones of the Caledonian foreland, southern Sweden.
139. Eriksson, Mårten, 2001: Bedömning av föroreningsspridning kring en nedlagd bensinstation i Karlaby, sydöstra Skåne.
140. Ljung, Karl, 2001: A paleoecological study of the Pleistocene-Holocene transition in the Kap Farvel area, South Greenland.
141. Åkesson, Cecilia, 2001: Undersökning av grundvattenförhållanden i området kring Östra Vemmerlöv, Simrishamns kommun, sydöstra Skåne.
142. Bermin, Jonas, 2001: Modelling Mössbauer spectra of biotite.
143. Mansurbeg, Howri, 2001: Modelling of reservoir quality in quartz-rich sandstones of the Lower Cretaceous Bentheim sandstones, Lower Saxony Basin, NW Germany.
144. Hermansson, Tobias, 2001: Sierggavággeskollans strukturgeologiska utveckling; nyckeln till Sareks berggrundsgeologi.
145. Veres, Daniel-Stefan, 2001: A comparative study between loss on ignition and total carbon analysis on Late Glacial sediments from Atteköps mosse, southwestern Sweden, and their tentative correlation with the GRIP event stratigraphy.
146. Ahlberg, Tomas, 2001: Hydrogeologisk undersökning samt sårbarhetskartering av området kring tre bergborrade grundvattenanläggningar i Simrishamns kommun.
147. Boman, Daniel, 2001: Tektonostratigrafi och deformationsrelaterad metamorfos i norra Kebnekaisefjällen, Skandinaviska Kaledoniderna.
148. Olsson, Stefan, 2002: The geology of the Portobello Peninsula; proposal of a saturated to oversaturated lineage within the Dunedin Volcano, New Zealand.
149. Molnos, Imre, 2002: Petrografi och diagenes i den underkambriska lagerföljden i Skrylle, Skåne.
150. Malmborg, Pär, 2002: Correlation between diagenesis and sedimentary facies of the Bentheim Sandstone, the Schoonebeek field, The Netherlands.
151. Jonsson, Henrik, 2002: Permeability variation in a tidal Jurassic deposit, Höganäs basin, Fennoscandian Border Zone
152. Lundgren, Anders, 2002: Seveskollorna i nordöstra Kebnekaise, Kaledoniderna: metabasiter, graniter och ögongnejser.
153. Sultan, Lina, 2002: Reconstruction of fan-shaped outwash in front of the Mýrdalsjökull ice cap, Iceland: Architecture and style of sedimentation.
154. Rimša, Andrius, 2002: Petrological study of the metamafic rocks across the Småland-Blekinge Deformation Zone
155. Lund, Magnus, 2002: Anti-slope scarp investigation at Handcar Peak, British Columbia, Canada.